14

Breast CAD (Computer Aided Detection) in FFDM (Full Field Digital Mammography)

Nachiko Uchiyama
Research Center for Cancer Prevention and Screening,
National Cancer Center, Tsukiji,
Chuo-Ku, Tokyo,
Japan

1. Introduction

In this chapter, firstly, the author describes the differences between CAD for analog mammography and FFDM with reference to clinical workflow and physical characteristics, and secondly, addresses how the detection performance of CAD can differ in accordance with image quality utilizing different FFDM systems, including future possibilities of breast CAD.

2. Difference between CAD with analog mammography and with digital mammography in clinical workflow

With CAD and analog mammography the CAD device is a single, independent device (Figure 1). The quality and quantity of image data depends on the film and the digitizer. It is easy to collect and analyze digital data through a film digitizer and the CAD system is an independent machine mainly developed by a venture company.

On the other hand, with CAD and digital mammography, it is necessary to collect so-called raw digital data from an acquisition system. To develop CAD software, it is necessary to work in conjunction with acquisition systems. Furthermore, CAD is an independent instrument with analog mammography; on the other hand, with digital mammography, CAD will be one of the interpretation functions of the reading workstation. For the most effective utilization, it is necessary to integrate CAD well with the reading workstation workflow.

Therefore, to disseminate CAD with digital mammography, we should take into consideration how to organize complete systems, including acquisition systems, reading workstations, and network systems. If the acquisition system and the reading workstation are made by the same maker, we can transfer raw image data from the acquisition system to the CAD server, and indicate Structure Report (SR) on the monitors at the reading workstation without any problems. On the other hand, when the makers are different, it may be a problem (Figure 2). For most effective utilization, it is necessary to integrate CAD well into the reading workstation workflow [1].

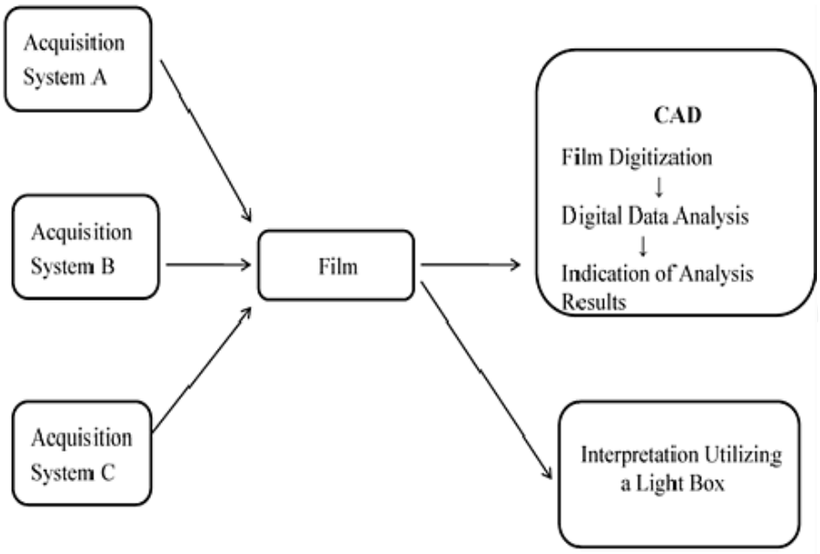

Fig. 1. Example of the Workflow of the CAD System Using Analog Mammography.

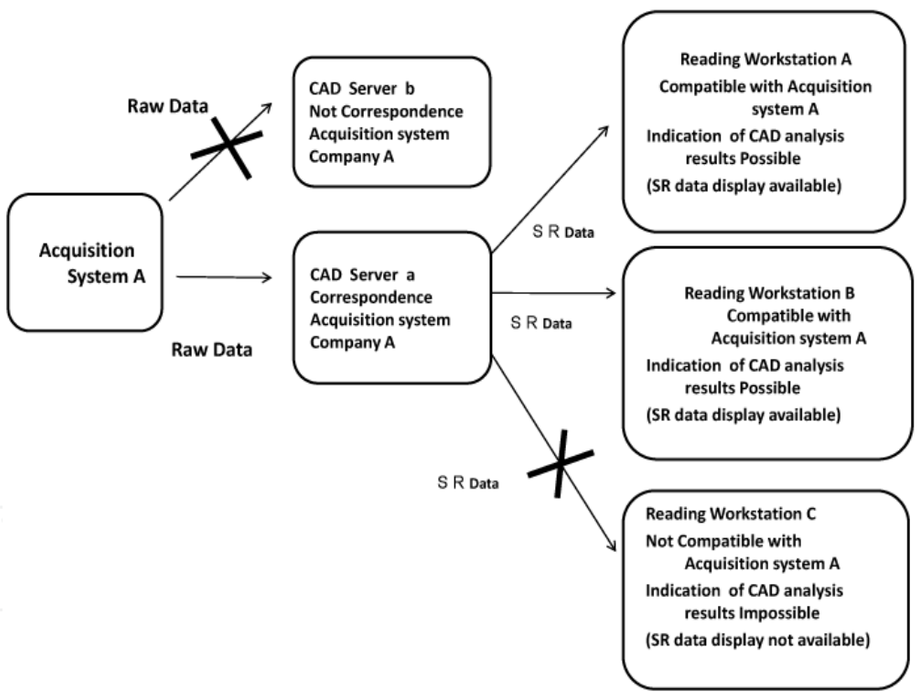

SR: Structure Report
CAD analyzes raw data from the acquisition system in a CAD server and refers the indication of CAD results to a reading workstation.
The quality and quantity of image data depends on the acquisition system. The operating system consists of three steps: (1) an acquisition system, (2) a CAD server, and (3) a reading work station. The number of makers of CAD systems that correspond to each acquisition system is limited. It is necessary to confirm before installation whether the reading workstation can display CAD analysis results.

Fig. 2. Example of the Workflow of the CAD System Using Digital Mammography.

3. How can image quality affect the detection performance of breast CAD in FFDM?

Purpose

At present, CAD, dedicated to digital mammography, analyzes the raw imaging data and detects candidate lesions including masses and microcalcifications. As for the physical characteristics, regarding the linear attenuation coefficient for breast tissue, the differential value between breast tissue and calcification is larger than the differential value between breast tissue and mass. In the raw imaging data, mass lesions have relatively localized large areas with a smaller number of photon counts compared to surrounding breast tissue. CAD analyzes the characteristics and detects the area as a candidate mass lesion. The raw imaging data is inverted and the mass lesion is recognized clinically as a localized high density area compared to background breast tissue density. In the raw imaging data, on the other hand, the images with microcalcification lesions have localized small and clustered areas with a smaller number of photon counts compared to the background breast tissue. CAD analyzes the characteristics and detects the area as a candidate microcalcification lesion. The raw imaging data is inverted and the microcalcification lesions are recognized clinically as small and clustered areas with higher density compared to the background breast tissue density. According to the background, CAD, dedicated to FFDM, can be directly affected by the physical characteristics of the raw imaging data. Unlike the raw imaging data on hard copy, utilizing digitizers for CAD processing in the analog system by groups, in units of 8-10 bits, the raw imaging data for CAD processing in FFDM are analyzed by groups, in units of 12-14 bits, which has a much more dynamic range compared to digitized hard copy data in the analog system. According to the background, in FFDM, there are more opportunities to apply a combination of anode/filters such as W/Rh that allows us to decrease the radiation dose while keeping higher image quality in CNR (Contrast to Noise Ratio), compared to the images using Mo/Mo and Mo/Rh in the analog system [2].The raw imaging data for CAD processing with FFDM can be more strongly influenced by the different contrast and image sharpness in clinical images, compared to the CAD dedicated to an analog system. Accordingly, the detection pattern in CAD can vary even in clinical cases. The author evaluated the variety of detection performance of CAD, utilizing two different FFDM systems with reference to analysis of physical characteristics such as CNR and spectral analysis of anode/filters. This study was conducted to retrospectively evaluate the variation of CAD performance according to different radiation exposure parameters [3,4]

4. Materials and methods

This study was conducted as part of research that was approved by the IRB at our institute on June 12th in 2007. All patients that were recruited for this study gave informed consent. The clinical cases in this study were selected from screening mammograms taken from June 12th in 2007 to December 24th in 2009. Clinical image data were acquired by two different FFDM systems. One was an a-Se FFDM system with a spatial resolution of 70ìm (System A) and imaging data were acquired from June 12th in 2007 to November 24th in 2008. Another was an a-Se FFDM system with a spatial resolution of 85ìm (System B) and imaging data were acquired from December 7th in 2008 to December 24th in 2009. Mammograms were diagnosed as BI-RADS category 1 or 2 by double-reading and breast ultrasound was performed in each case and diagnosed as a normal or a benign case. The total number of

cases was 1140 cases in System A and 1178 cases in System B. The median patient age was 59.8 years old (range 40-75 years old) in System A and 60.0 years old (range 40-88 years old) in System B. To optimize radiation exposure parameters in clinical images, we measured CNR (Contrast to Noise Ratio) in accordance with EUREF (European Guidelines for Quality Assurance in Breast Cancer Screening and Diagnosis) guide lines simulating breast thickness, utilizing PMMA phantoms (20-70mm) and radiation exposure parameters, kV (24-34kV) and combinations of anode/filters (Mo/Mo, Mo/ Rh, and W/Rh). In addition, we performed spectral analysis of anode/filters (Mo/Mo, Mo/ Rh, and W/Rh) regarding both FFDM systems. A CAD dedicated to the FFDM systems was applied for the purpose of review and was verified, regarding detection areas, with reference to the diagnostic reports of the mammogram and ultrasound. The same CAD algorithm was utilized for the two FFDM systems.

5. Results

We optimized radiation exposure parameters in a clinical setting with reference to the results of the CNR analysis and dosimetry in accordance with EUREF Guidelines [5] (Fig.3.).

In System A, under 20mm breast thickness, the combination of 24kV with Mo/Mo was selected; from 21m to 30mm breast thickness, the combination of 26kV with Mo/Mo was selected; from 31mm to 40mm breast thickness, the combination of 28kV with Mo/Mo was selected; from 41to 60mm, the combination of 30kV with W/Rh was selected; from 61mm to 70mm, the combination of 32kV with W/Rh was selected; and above 70mm, the combination of 34kV with W/Rh was selected (Fig.4-5).

$$CNR = \frac{\text{mean pixel value (signal)-mean pixel value (background)}}{\sqrt{\frac{SD\,(signal)^2 + SD\,(background)^2}{2}}}$$

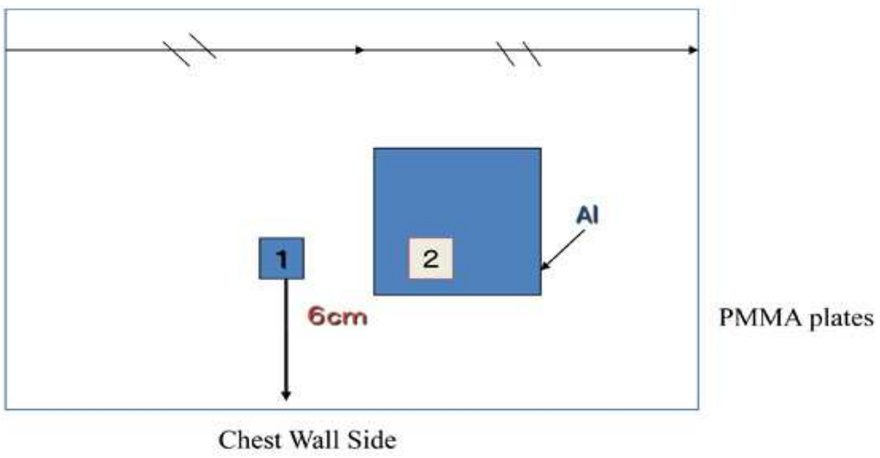

SD; Standard Deviation

Fig. 3. CNR Measurements in Accordance with EUREF.

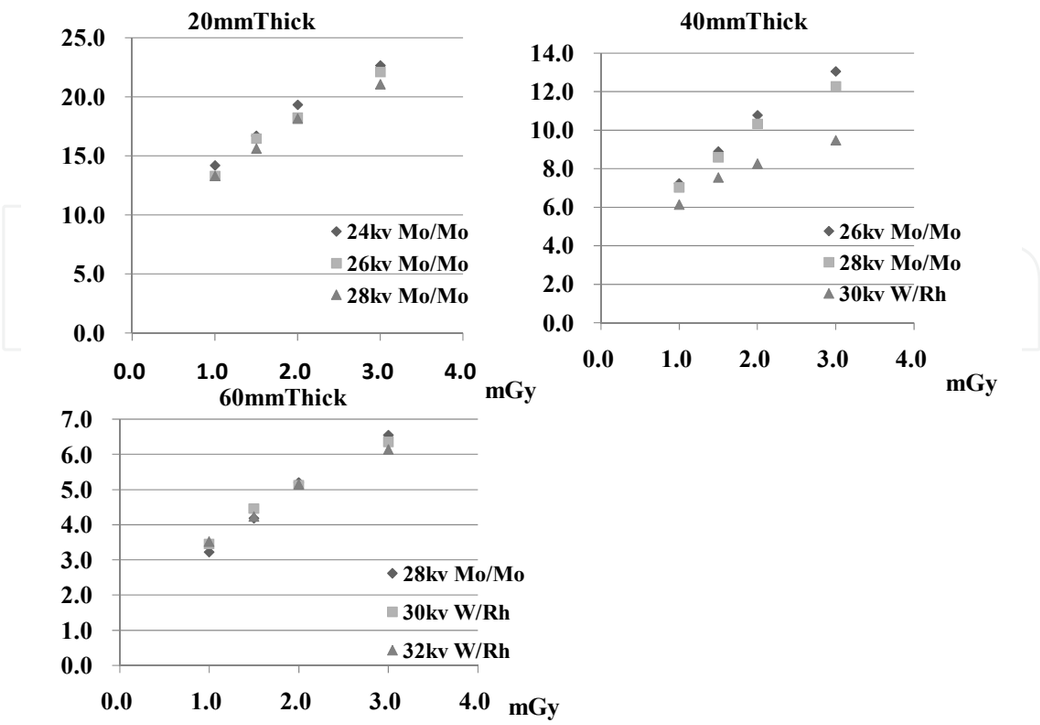

Fig. 4. CNR Analysis: 20mm, 40mm, and 60mmThick PMMA Phantoms in System A.

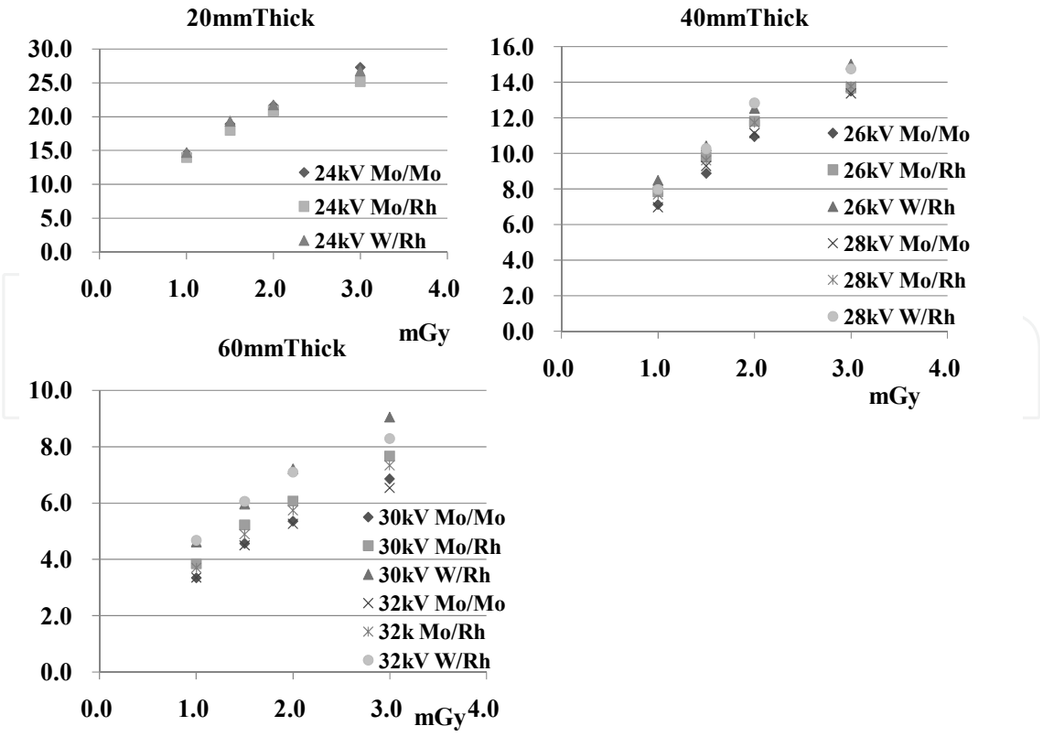

Fig. 5. CNR Analysis: 20mm,40mm,and 60mm Thick PMMA Phantoms in System B.

CAD detected relatively dense areas as false-positive masses at a rate of 9.8% (448/4560 images) and fibrous tissue as false-positive microcalcifications at a rate of 0.7% (34/4560 images).

In the cases utilizing 24-28kV Mo/Mo, CAD detected masses as false positives more frequently at a rate of 12.7% (279/2196 images), compared to the cases utilizing 30-34 kV W/Rh which detected false positives at a rate of 7.1% (169/2364 images). There was a statistically significant difference ($P=0.008<0.05$) between the two different combinations of anode/filters. CAD detected more false-positive masses in the cases utilizing the combinations with Mo/Mo in comparison with the cases utilizing the combinations with W/Rh. On the other hand, in the cases utilizing 30-34kV W/Rh, CAD detected false-positive microcalcifications more frequently at a rate of 1.1% (26/2364 images), compared to 0.4 % (8/2196 images) detected utilizing 24-28kV Mo/Mo. There was a statistically significant difference ($P=0.022<0.05$) between the two combinations with different anode/filters. CAD detected more false-positive calcifications in the cases utilizing W/Rh in comparison with the cases utilizing Mo/Mo (Table 1a.). In System B, under 25mm breast thickness, the combination of 24kV with W/Rh was selected; from 26m to 35mm breast thickness, the combination of 26kV with W/Rh was selected; from 36mm to 45mm breast thickness, the combination of 28kV with W/Rh was selected; from 46 to 55mm, the combination of 30kV with W/Rh was selected; and above 56mm, the combination of 32kV-34kV with W/Rh was selected. CAD detected false-positive masses at a rate of 2.7% (129/4712 images) and false-positive microcalcifications at a rate of 0.8% (37/4712 images) in total. With 24kV, CAD detected false-positive masses at a rate of 1.0% (5/500 images) and false-positive microcalcifications at a rate of 1.2% (6/500 images). With 26kV, CAD detected false-positive masses at a rate of 3.3% (32/960 images) and false-positive microcalcifications at a rate of 0.7% (7/960 images). With 28kV, CAD detected false-positive masses at a rate of 3.3% (48/1460 images) and false-positive microcalcifications at a rate of 1.2% (18/1460 images).With 30kV, CAD detected false-positive masses at a rate of 1.4% (16/1128 images) and false-positive microcalcifications at a rate of 0.5% (6/1128 images). With 32-34kV, CAD detected false-positive masses at a rate of 4.2% (28/664images) and 0% (0/664 images) false-positive microcalcifications. There was no significant difference among different kV levels with the same combination of anode/filters in System B ($P>0.05$) (Table 1b.).

Regarding spectral analysis of anode/filters, in System A, Mo/Mo and W/Rh demonstrated different spectrum characteristic curves. In addition, the two systems showed different spectrum characteristic curves with W/Rh and the peak value in System B with W/Rh was shown at a higher kV level compared to System A (Fig.6-7).

6. Discussion

At present, CAD dedicated to digital mammography analyzes the raw imaging data and detects the candidate lesions including masses and microcalcifications. As for the physical characteristics, regarding the linear attenuation coefficient for breast tissue [6], the differential value between breast tissue and calcification is larger than the differential value between breast tissue and mass (Table2).

Mass lesions have relatively localized large areas with a smaller number of photon counts compared to surrounding breast tissue in the raw imaging data. CAD analyzes the

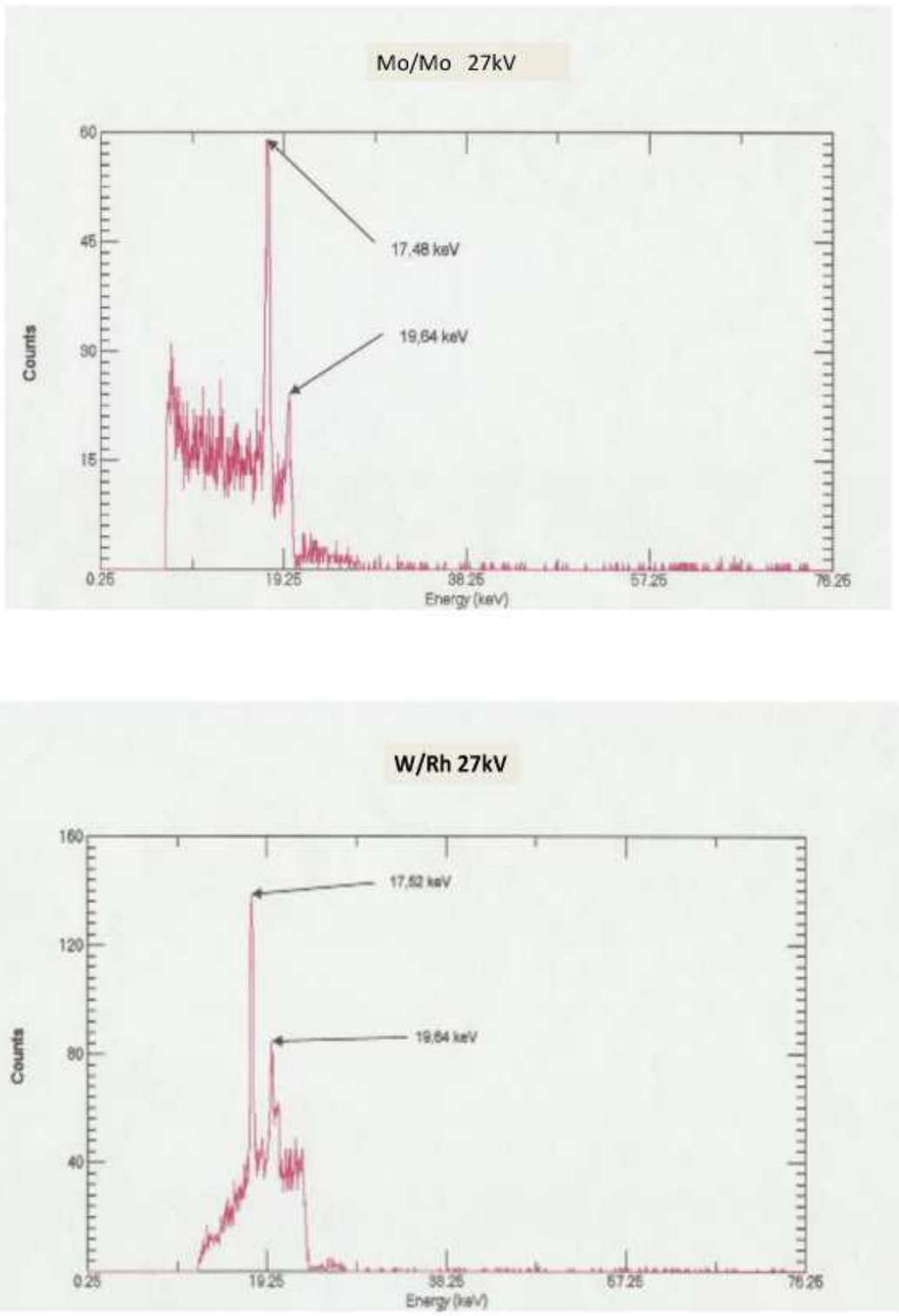

Fig. 6. Spectra of Mo/Mo and W/Rh in System A.

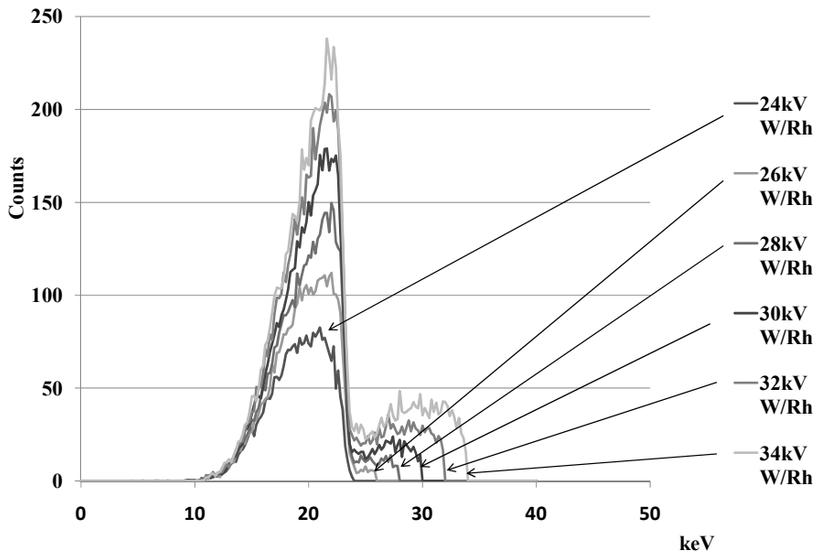

Fig. 7. Spectrum of W/Rh in System B.

Table1a.

	FP Mass		FP Microcalcifications	
24-28kV Mo/Mo	12.7% (279/2196)	P=0.008<0.05	0.4% (8/2196)	P=0.022<0.05
30-34kV W/Rh	7.1% (169/2364)		1.1% (26/2364)	
Total	9.8% (448/4560)		0.7% (34/4560)	

Table1b.

	FP Mass		FP Microcalcifications	
24kV W/Rh	1.0% (5/500)	P>0.05	1.2% (6/500)	P>0.05
26kV W/Rh	3.3% (32/960)		0.7% (7/960)	
28kV W/Rh	3.3% (48/1460)		1.2% (18/1460)	
30kV W/Rh	1.4% (16/1128)		0.5% (6/1128)	
32-34kV W/Rh	4.2% (28/664)		0% (0/664)	
Total	2.7% (129/4712)		0.8% (37/4712)	

Table 1. Clinical Radiation Exposure Setting of System A (Table 1a) and System B. (Table1b) regarding Frequency of False Positives (FPs) using CAD.

	Linear Attenuation Coefficient(cm^{-1})
Breast Tissue	0.8
Fatty Tissue	0.45
Skin	0.8
Mass	0.85
Calcification	12.5

Table 2. Linear Attenuation Coefficient of Breast Tissue at 20keV [6].

characteristics and detects the area as a candidate mass lesion. The raw imaging data is inverted and the mass lesion is recognized clinically as a localized high density area compared to background breast tissue density. On the other hand, the images with microcalcification lesions have localized small and clustered areas with a smaller number of photon counts compared to the background breast tissue in the raw imaging data. CAD analyzes the characteristics and detects the area as a candidate microcalcification lesion. The raw imaging data is inverted and the microcalcification lesions are recognized clinically as small and clustered areas with higher density compared to the background breast tissue density. According to the background, CAD dedicated to digital mammography can be directly affected by the physical characteristics of the raw imaging data. In this study, in System A, CAD detected more false positive masses with 24-28Kv Mo/Mo compared to those detected with 30-34Kv W/Rh. According to spectral analysis, Mo/Mo acquires a smaller number of photons compared to W/Rh . The raw imaging data with Mo/Mo has a relatively narrow range of photon counts and the differentials in the photon counts between background breast tissue and mass can be small. As a result, CAD can detect more false positive masses compared to imaging with W/Rh. On the other hand, CAD detected more false positive microcalcifications with 30-34Kv W/Rh compared to the number detected with 24-28Kv Mo/Mo (Fig.8-9).

This could be a result of the characteristics of W/Rh which can acquire a larger number of photons compared to Mo/Mo. Images with W/Rh have a much wider range of photon counts and the differential value of photon counts between background breast tissue and microcalcifications is large. As a result, imaging data with W/Rh can detect candidate microcalcification lesions with more sensitivity than imaging with Mo/Mo. Even with the same combination of anode/filters, the CAD in System A with 30-34kV W/Rh detected more false positive masses compared to System B with 30-34kV W/Rh.CAD results may differ even when the same system is used, according to which combination of anode/filter is used. On the other hand, CAD results may differ when different systems are used, even though the same combination of anode/filter is used. According to spectral analysis, the spectrum of W/Rh used in System A shows greater similarity to the spectrum of Mo/Mo than the spectrum of W/Rh used in System B. As a result, CAD detected more false positives using W/Rh with System A compared to System B. The CAD performance was

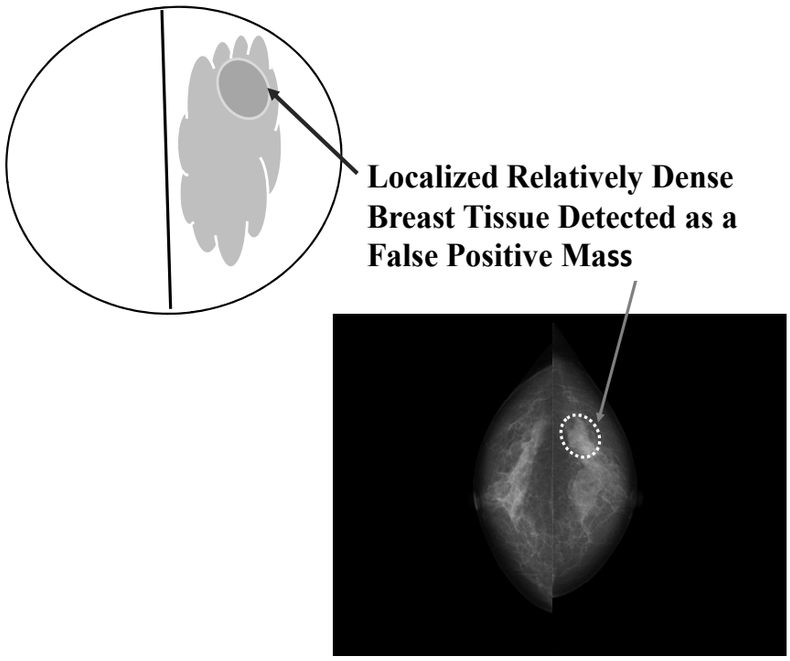

Fig. 8. Example Case with a False Positive Mass Marked by CAD.

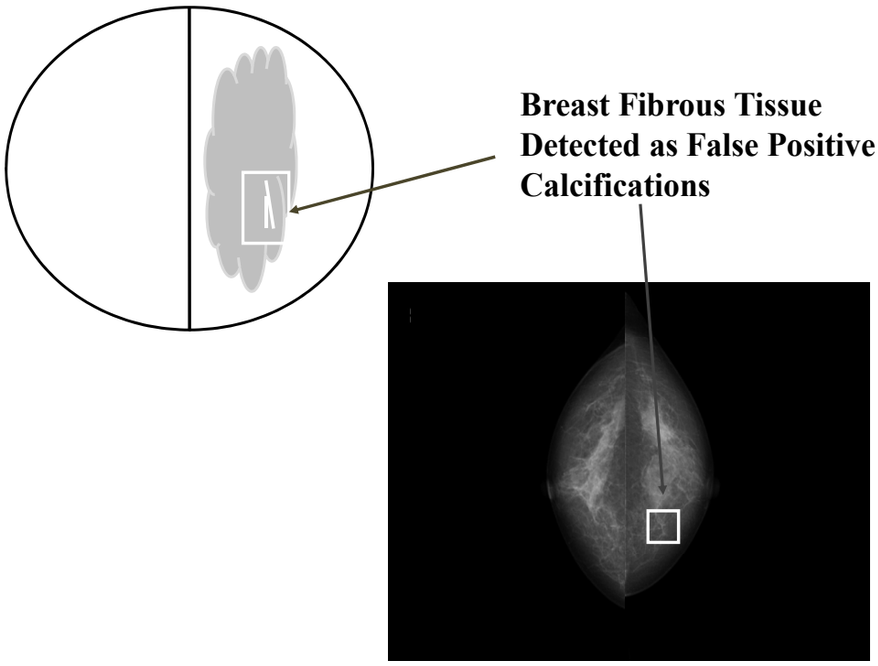

Fig. 9. An Example Case with False Positive Calcifications Marked by CAD.

affected by the difference in image quality produced by different radiation exposure parameters of the different anode/filters within one system and by differences in the two systems. In FFDM, CAD algorithms should be considered to vary depending on the image acquisition systems. In addition, recently, new breast image acquisition technologies, as well as digital breast tomosynthesis and dual-energy mammography, have been developed and have started to be acquired for breast diagnosis. These image acquisition approaches, utilizing new CAD techniques, will be capable of accurate volumetric measuring of breast density and microcalcifications, differently from conventional 2D images [7]-[9]. The results of this study imply that we should take into consideration the importance of analyzing physical characteristics with CAD, according to the different image quality with systems dedicated to new image acquisition technologies.

7. Conclusion

In this section, the author addresses the issue that CAD performance is affected by the difference in image quality produced by different radiation exposure parameters of the different anode/filters within one system and by differences in the two systems; also variations in CAD algorithms utilizing FFDM should be taken into account.

8. Acknowledgment

This study was supported by Grant-in-Aid for Scientific Research (C) (No. 23591810) in Japan.

9. References

[1] Uchiyama N.: Current status of CAD utilizing digital mammography in Japan. Breast Cancer. 2010; 17(3) 169-179.

[2] Toroi, P., Zanca, F., Young, K. C. et al.: Experimental Investigation on the Choice of the Tungsten/Rhodium Anode/Filter Combination for an Amorphous Selenium-Based Digital Mammography System. 2007.Eur. Radiol.17,2368-23752.

[3] Uchiyama N, Stoeckel J, Otsuka K, et al.:How Can Image Quality Affect the Detection Performance of Breast CAD (Computer Aided Detection) in FFDM (Full Field Digital Mammography)? A Comparative Study with Two Different FFDM Systems. Digital Mammography. 2010. 6136 288-295.

[4] Uchiyama N,Stoeckel J, Otsuka K. et al.:How Can Image Quality Affect the Detection Performances of Breast CAD (Computer Aided Detection) in FFDM (Full Field Digital Mammography)? 2009. Int J CARS;4:357-358.

[5] EUREF; European Guidelines for Quality Assurance in Breast Cancer Screening and Diagnosis 4th Edition 2006.

[6] Hammerstein, G.R., Miller, D.W., et al; Absorbed Radiation Dose in Mammography. Radiol. 1979. 130:485-491.

[7] Reiser I., Nishikawa R. M., Giger M. L. et.al. Computerized Detection of Mass Lesions in Digital Breast Tomosynthesis Images Using Two- and Three Dimensional Radial Gradient Index Segmentation.2004. Technol. Cancer Res. Treat. 3, 437–441

[8] Chan H.P., Wei J., Zhang Y., et.al. Computer-Aided Detection of Masses in Digital Tomosynthesis Mammography: Comparison of Three Approaches. 2008. Med. Phys. 35, 4087-4095.

[9] Ducote J. L. and Molloi S.. 2008. Quantification of Breast Density with Dual Energy Mammography: A Simulation Study.2008.Med. Phys. 35, 5411–5418.

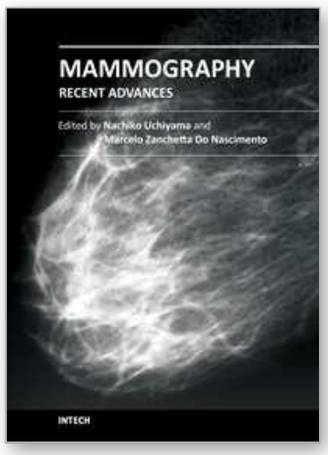

Mammography - Recent Advances
Edited by Dr. Nachiko Uchiyama

ISBN 978-953-51-0285-4
Hard cover, 418 pages
Publisher InTech
Published online 16, March, 2012
Published in print edition March, 2012

In this volume, the topics are constructed from a variety of contents: the bases of mammography systems, optimization of screening mammography with reference to evidence-based research, new technologies of image acquisition and its surrounding systems, and case reports with reference to up-to-date multimodality images of breast cancer. Mammography has been lagged in the transition to digital imaging systems because of the necessity of high resolution for diagnosis. However, in the past ten years, technical improvement has resolved the difficulties and boosted new diagnostic systems. We hope that the reader will learn the essentials of mammography and will be forward-looking for the new technologies. We want to express our sincere gratitude and appreciation?to all the co-authors who have contributed their work to this volume.

InTech Europe
University Campus STeP Ri
Slavka Krautzeka 83/A
51000 Rijeka, Croatia
Phone: +385 (51) 770 447
Fax: +385 (51) 686 166
www.intechopen.com

InTech China
Unit 405, Office Block, Hotel Equatorial Shanghai
No.65, Yan An Road (West), Shanghai, 200040, China
中国上海市延安西路65号上海国际贵都大饭店办公楼405单元
Phone: +86-21-62489820
Fax: +86-21-62489821

IntechOpen